Journal of Applied Physiology

Mechanical deformation of neutrophils into narrow channels induces pseudopod projection and changes in biomechanical properties

Belinda Yap and Roger D. Kamm

Journal of Applied Physiology 98:1930-1939, 2005. First published Jan 7, 2005;
doi:10.1152/japplphysiol.01226.2004

You might find this additional information useful...

This article cites 38 articles, 24 of which you can access free at:
http://jap.physiology.org/cgi/content/full/98/5/1930#BIBL

This article has been cited by 1 other HighWire hosted article:
Cytoskeletal remodeling and cellular activation during deformation of neutrophils into narrow channels
B. Yap and R. D. Kamm
J Appl Physiol, December 1, 2005; 99 (6): 2323-2330.
[Abstract] [Full Text] [PDF]

Updated information and services including high-resolution figures, can be found at:
http://jap.physiology.org/cgi/content/full/98/5/1930

Additional material and information about ***Journal of Applied Physiology*** can be found at:
http://www.the-aps.org/publications/jappl

This information is current as of December 27, 2005 .

Journal of Applied Physiology publishes original papers that deal with diverse areas of research in applied physiology, especially those papers emphasizing adaptive and integrative mechanisms. It is published 12 times a year (monthly) by the American Physiological Society, 9650 Rockville Pike, Bethesda MD 20814-3991. Copyright © 2005 by the American Physiological Society. ISSN: 8750-7587, ESSN: 1522-1601. Visit our website at http://www.the-aps.org/.

Downloaded from jap.physiology.org on December 27, 2005

J Appl Physiol 98: 1930–1939, 2005.
First published January 7, 2005; doi:10.1152/japplphysiol.01226.2004.

HIGHLIGHTED TOPIC | *Biomechanics and Mechanotransduction in Cells and Tissues*

Mechanical deformation of neutrophils into narrow channels induces pseudopod projection and changes in biomechanical properties

Belinda Yap[1,2] and Roger D. Kamm[2]

[1]*Harvard-MIT Division of Health Sciences and Technology, and* [2]*Department of Mechanical Engineering and Biological Engineering Division, Massachusetts Institute of Technology, Cambridge, Massachusetts*

Submitted 1 November 2004; accepted in final form 4 January 2005

Yap, Belinda, and Roger D. Kamm. Mechanical deformation of neutrophils into narrow channels induces pseudopod projection and changes in biomechanical properties. *J Appl Physiol* 98: 1930–1939, 2005. First published January 7, 2005; doi:10.1152/japplphysiol.01226.2004.—Neutrophils traversing the pulmonary microcirculation are subjected to mechanical stimulation during their deformation into narrow capillaries. To better understand the time-dependant changes caused by this mechanical stimulus, neutrophils were caused to flow into a microchannel, which allowed simultaneous visualization of cell morphology and passive rheological measurement by tracking the Brownian motion of endogenous granules. Above a threshold stimulus, mechanical deformation resulted in neutrophil activation with pseudopod projection. The activation time was inversely correlated to the rate of mechanical deformation experienced by the neutrophils. A reduction in shear moduli was observed within seconds after the onset of the mechanical stimulus, suggesting a sudden disruption of the neutrophil cytoskeleton when subjected to mechanical deformation. However, the magnitude of the reduction in moduli was independent of the degree of deformation. Recovery to nearly the initial values of viscoelastic moduli occurred within 1 min. These observations confirm that mechanical deformation of neutrophils, similar to conditions encountered in the pulmonary capillaries, is not a passive event; rather, it is capable of activating the neutrophils and enhancing their migratory tendencies.

viscoelasticity; cell activation; multiple-particle tracking; microfluidics

NEUTROPHILS OFTEN ENCOUNTER narrow capillary segments during their transit through the pulmonary and systemic microcirculations. Because neutrophil diameters (6–8 μm) often exceed the diameter of a pulmonary capillary (2–15 μm) (5), neutrophils would almost certainly have to deform in passing from arteriole to venule, particularly in the pulmonary capillary bed, where it has been estimated that a typical flow pathway encompasses 50–100 such capillary segments (13, 14). Measurements of neutrophil shape showed that neutrophils in capillaries are elongated, whereas those in arterioles are nearly spherical, thus confirming the view that neutrophils deform when they encounter narrow capillary segments (5, 12).

Mechanical forces have been recognized to play an important role in modulating the behavior and function of cardiovascular cells in health and disease (15, 17). Although the effects of mechanical stimuli on cells have been a topic of extensive research, much of the focus has been on endothelial cells in the context of atherosclerotic disease. Neutrophil, and leukocyte activity in general, is assumed to be mediated in large part by biochemical factors, with effects from mechanical stimulation often ignored. However, recent studies have shown that leukocytes are sensitive to fluid shear stress, which can influence their degree of substrate adhesion and the formation of pseudopods and reduce their cytoskeletal stiffness (2, 22, 28). Similarly, the mechanical deformation of neutrophils into narrow pulmonary capillaries, initially considered to be a passive process, is now recognized to enhance adhesiveness to ICAM-1 through upregulation of CD11b/CD18, reorganizing and stabilizing the cytoskeleton, and increasing free intracellular Ca^{2+} concentration (21). Consequently, neutrophils likely have the capability of sensing mechanical force or deformation and altering their rheological properties in response. Despite the importance of these effects in the microcirculation, no rheological studies have yet been conducted subjecting neutrophils to the deformations they experience while traversing the pulmonary circulation. Interestingly, one of the established techniques for measuring the viscoelastic properties of neutrophils, the micropipette aspiration method, involves deformation of the cell under a fixed suction pressure into a narrow micropipette (9, 29, 32, 33). This technique mimics the flow condition that the cell experiences while deforming into a pulmonary capillary. The rheological properties deduced from this technique, however, assume that the neutrophil remains passive during deformation and, hence, that its rheology is unchanged when drawn into the pipette. Indeed, some of these micropipette experiments showed some indications of neutrophil activation attributed to mechanical deformation of the cell (8).

In such cases for which mechanical deformation by external forces give rise to a change in rheological properties, it is advantageous to seek methods of measurement that avoid cell manipulation. Multiple-particle-tracking microrheology (23, 24, 34) offers a solution because this method is able to noninvasively measure the local viscoelasticity by monitoring the Brownian motion of endogeneous granules present in the cytoplasm of the cell. A similar technique has been applied to locomoting neutrophils, with active manipulation of a granule using an optical trap (37, 38). To examine the effects of mechanical deformation on the behavior and rheological properties of the neutrophils in the pulmonary capillaries, we used microfabrication techniques (27, 35) to construct an in vitro

Address for reprint requests and other correspondence: R. D. Kamm, Dept. of Mechanical Engineering and Biological Engineering Division, Massachusetts Institute of Technology, 77 Massachusetts Ave. NE47-321, Cambridge, MA 02139 (E-mail: rdkamm@mit.edu).

The costs of publication of this article were defrayed in part by the payment of page charges. The article must therefore be hereby marked "*advertisement*" in accordance with 18 U.S.C. Section 1734 solely to indicate this fact.

8750-7587/05 $8.00 Copyright © 2005 the American Physiological Society

Journal of Applied Physiology

Downloaded from jap.physiology.org on December 27, 2005

polydimethylsiloxane (PDMS) system with dimensions comparable to the pulmonary capillaries. PDMS being optically transparent enabled direct observation of the neutrophil morphology and simultaneously allowed us to employ the technique of multiple-particle-tracking microrheology to directly measure the viscoelastic properties of the cell.

MATERIALS AND METHODS

Design and fabrication of microfluidic device. The design of the microchannel used to mimic a pulmonary capillary and the connecting reservoirs is shown in Fig. 1. A master for this design was fabricated on silicon wafer using the technique of two-level photolithography (20) and subsequently used for replica molding in PDMS (18). Figure 2 shows the finished microfluidic system. The details of the fabrication process can be found in the APPENDIX.

Macrofluidic system setup. Pressure differential was imposed across the microchannel by varying the difference in height of water between the upstream and downstream macroreservoirs (Fig. 3). Two upstream macroreservoirs were used: a high-pressure (~60 cmH_2O) reservoir for purging and cleaning and a low-pressure reservoir for neutrophil perfusions. The upstream low-pressure macroreservoir was attached to a linear translation stage (Edmund Optics, Barrington, NJ) and mounted on a linear slide (Rapid Advance Unislides, Velmex, Bloomfield, NY) enabling both fine-scale (0.01-mm steps) and coarse-scale (1-mm steps) adjustment. A syringe attached to the second port of the upstream microfluidic reservoir allowed the introduction of fluid or cells into the device.

Neutrophil isolation. Human venous blood was drawn from healthy volunteers by venipuncture into syringes containing 0.1 M sodium citrate as an anticoagulant. The isolation was in accordance with a protocol approved by the Massachusetts Institute of Technology Committee on Use of Humans as Experimental Subjects. Neutrophils were isolated from mononuclear cells by density gradient centrifugation on Histopaque 1077 (Sigma-Aldrich, St. Louis, MO) at 175 *g* for 30 min at room temperature. The supernatant plasma layer was collected for later use in the experiment. The mononuclear layer was carefully removed, and the remaining neutrophil and red blood cell layers were resuspended first in an equal volume of HBSS without Ca^{2+} or Mg^{2+} (Invitrogen, Carlsbad, CA) and then in a 1:1 dilution of dextran (average molecular weight 500,000, 2% final concentration, Pharmacia, Peapack, NJ). Red blood cells were allowed to sediment for 30 min at room temperature, after which, the neutrophil-rich supernatant was collected, rinsed with HBSS, and centrifuged at 175 *g* for 5 min at room temperature. Residual red blood cells were removed by hypotonic lysis. Isotonicity was restored by the addition of 45 ml of HBSS without Ca^{2+} or Mg^{2+}, and the sample was then centrifuged at 175 *g* for 5 min at room temperature. The isolated neutrophils were resuspended in either HBSS without Ca^{2+} or Mg^{2+} only, or in medium (HBSS without Ca^{2+} or Mg^{2+} + 2% autologous plasma). After counting, the neutrophil concentration was adjusted to 1.0×10^6 cells/ml, and depending on experimental requirements the

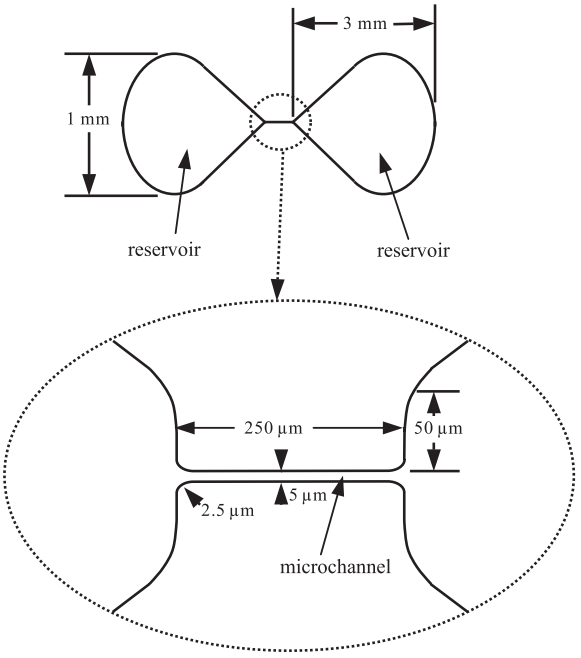

Fig. 1. Schematic showing design of the microchannel and its connecting reservoirs. The microchannel section is enlarged to highlight the channel geometry. The important channel dimensions are: length of 250 μm, width of 5 μm, and inlet radius of curvature of 2.5 μm. Diagrams are not drawn to scale.

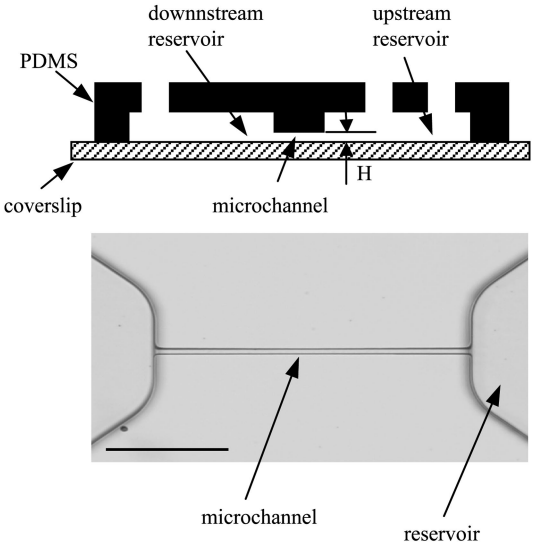

Fig. 2. *Top*: schematic diagram of the finished polydimethylsiloxane (PDMS) microfluidic device with 2 inlet and 1 outlet reservoir ports. The device is sealed on a glass coverslip. H represents the microchannel height, which is either 1.5 or 2.5 μm. Diagram is not drawn to scale. *Bottom*: image of microchannel molded from PDMS as seen under a light microscope. Scale bar, 100 μm.

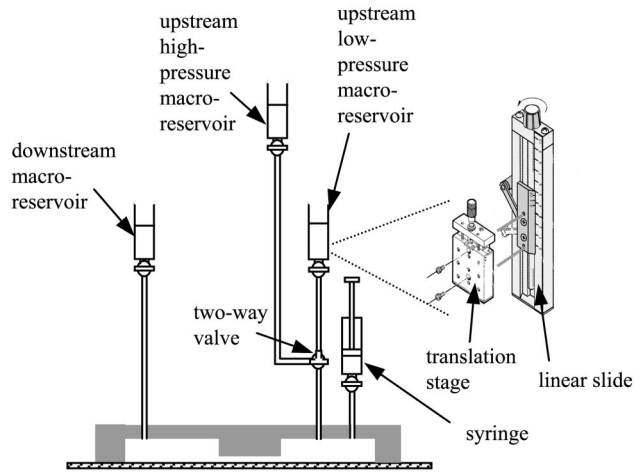

Fig. 3. Schematic showing the macrofluidic system setup and its connections to the microfluidic device. Refer to MATERIALS AND METHODS for explanation on the function of each of the system components.

Journal of Applied Physiology

Downloaded from jap.physiology.org on December 27, 2005

cells were kept either at room temperature or incubated in a 37°C water bath.

Optical microscopy. Neutrophils were observed using a differential interference contrast microscope (Eclipse TE2000, Nikon, Melville, NY) equipped with an oil immersion condenser lens [numerical aperature (NA) 1.4] and a ×100/1.4 NA Plan Apochromat objective lens. Images were acquired with a video camera (CCD-100, Dage-MTI, Michigan City, IN) and recorded onto a super-VHS tape at 30 frames/s with a cassette recorder (SVO-9500MD, Sony). The movies were then converted into digital form with a computer equipped with a frame-grabber card (Scion LG-3, Frederick, MD).

Deformation and trapping of neutrophils inside microchannel. The microfluidic device was first incubated with 1% pluronic F108 solution (PEO/PPO/PEO triblock copolymers, BASF, Mount Olive, NJ) in water for 2 h, which served to passivate the PDMS surface and deter cell adhesion (19). The device was then flushed with medium (HBSS without Ca^{2+} or Mg^{2+} + 2% autologous plasma) for 15 min. An objective heater (Bioptech, Butler, PA) set to 37°C was used for experiments at body temperature.

Neutrophils suspended in medium were then introduced into the upstream microfluidic reservoir. By setting the upstream two-way valve to open to the upstream high-pressure macroreservoir, the cells flowed quickly toward the microchannel entrance zone. In addition, yellow-green fluorescent 0.1-μm microspheres (carboxylate-modified polystyrene fluospheres, Molecular Probes), diluted in HBSS (without Ca^{2+} or Mg^{2+}) at a concentration of 5×10^8 beads/ml, were introduced into the upstream microfluidic reservoir and used to establish the zero-pressure difference, zero-flow condition.

Finally, the low-pressure macroreservoir was raised to impose the desired pressure differential across the channel, initiating a flow of neutrophils into the microchannel. Once a neutrophil had entered the microchannel, the low-pressure macroreservoir was returned to its initial height, which immediately stopped its flow through the channel.

Entrance time and time to pseudopod projection. Neutrophil behavior was recorded from the start of its deformation into the channel up to the formation of the first pseudopod projection either at the leading or trailing edge of the cell. The playback of the video recording allowed precise determination of neutrophil entrance time and the first observation of pseudopod projection. The entrance time was taken to be the interval between when the neutrophil leading edge touched the channel entrance (first contact) and when the trailing edge cleared the channel mouth after deformation. The time to pseudopod formation was defined as the time from first contact to the first appearance of the pseudopod projection.

Viscoelastic properties of the neutrophil evaluated using multiple-particle-tracking microrheology. Brownian motion of endogeneous granules inside the neutrophils was monitored using particle-tracking algorithms (3) written in the IDL software (Research Systems, Boulder, CO) from the instant the neutrophil was trapped in the microchannel until the observation of pseudopod projection. The focal plane for particle tracking was selected near the center of the microchannel to minimize wall effects. From the video images, the cytoplasm of the neutrophil was divided into two zones (Fig. 4): *zone 1* was just proximal to the nucleus, and *zone 2* was the remainder of the cytoplasm up to the cell tip. Granules in *zone 1*, as well as granules exhibiting obvious directed active movements in both zones, were excluded from particle tracking. In addition, only granules that appeared circular were selected for tracking, achieved by setting the computer algorithms to track particles with eccentricity of ≤0.3 (major and minor axis difference of <5%). Only particles that remained in focus for at least 30 frames were analyzed. Because of the high density of granules present in the neutrophil cytoplasm, all tracks performed by the computer algorithms were visually checked with the original video images to ensure that the same particle was followed throughout a particular track. From these particle trajectories, mean-square displacements, the frequency-dependent elastic modulus (G′), and loss modulus (G″) were computed according to the methods of Mason et al. (26). The shortest time lag of 1/30 s was chosen for these viscoelastic calculations because it gave the best statistical accuracy. The radius of a typical neutrophil granule was taken to be 300 nm (37) in these computations. Temporal changes in G′ and G″ were examined by performing independent analysis on 5-s time intervals.

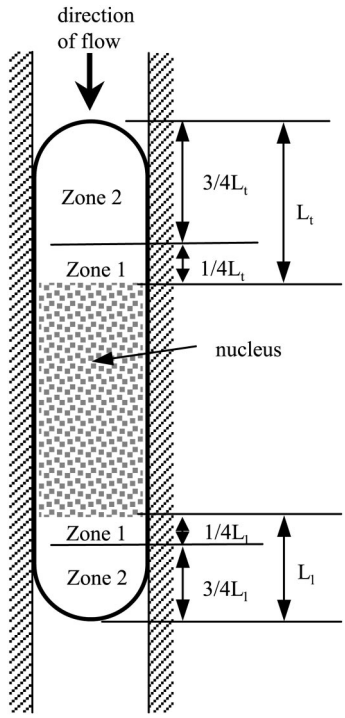

Fig. 4. Schematic diagram illustrating the division of the neutrophil cytoplasm into 2 regions; *zone 1*, proximal to the nucleus; and *zone 2*, distal from nucleus up to the cell leading or trailing edge. Only granules dispersed in *zone 2* were selected for particle tracking. L_l, length from nuclear boundary to the leading edge; L_t, length from nuclear boundary to the trailing edge.

As control, the multiple-particle-tracking technique was also performed on round passive neutrophils (Fig. 5*A*). Neutrophils suspended in medium were introduced into a small chamber formed between a glass slide and coverslip. Again, granules close to the nucleus were excluded from the particle track.

Studies were also performed on adherent and spread neutrophils (Fig. 5*B*) on a glass coverslip. Neutrophils suspended in HBSS without Ca^{2+} or Mg^{2+} were introduced into a glass slide and coverslip chamber as before. The absence of plasma in the suspension resulted in adhesion and spreading. Only granules in the cytoplasm that were located at least 2 μm away from the nucleus of the cell were tracked. Values obtained for G′ and viscosity (η) at 1 Hz were compared with published results of noninvasive intracellular measurement of neutrophils (37). Because the measurements were performed at a higher frequency to allow comparison with the published data, particles chosen for tracking were in focus for at least 100 frames.

Statistical analysis. All results are expressed as means ± SE. Comparisons of data were carried out using the paired, two-tailed Student's *t*-test, and findings that showed either $P < 0.05$ or $P < 0.01$ were considered significant.

RESULTS

Neutrophils were introduced into microchannels comprising two different cross-sectional dimensions; a larger cross-sectional area with dimensions of 5 μm in width and 2.5 μm in height, and a second smaller area with channel width of 5 μm

Journal of Applied Physiology

Downloaded from jap.physiology.org on December 27, 2005

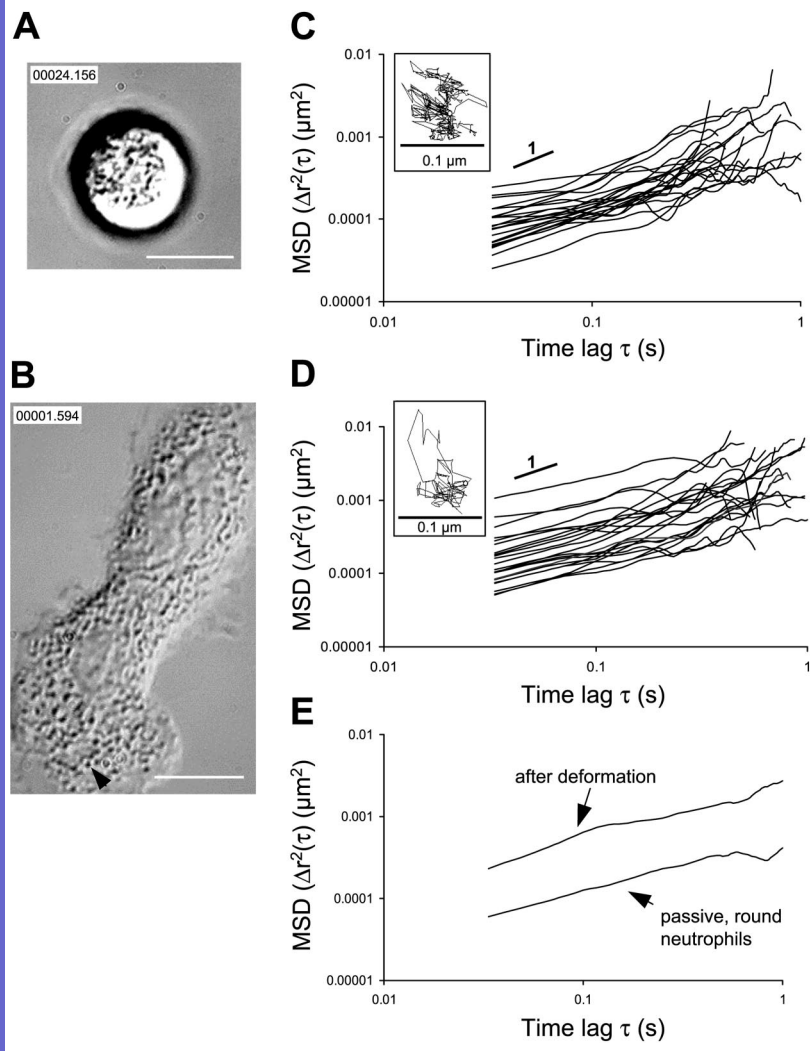

Fig. 5. *A*: image of a round, passive neutrophil. Clearly seen are the endogeneous granules in the cytoplasm of the cell. Scale bar, 5 μm. *B*: image of a neutrophil that had spread out on a coverslip showing many endogeneous granules dispersed throughout the cytoplasm. As described in MATERIALS AND METHODS, only granules located at least 2 μm away from the nucleus (an example is shown with an arrow) were tracked, whereas granules situated proximal to the nucleus were ignored in the tracking. Scale bar, 5 μm. *C*: individual mean-squared-displacement (MSD) traces of randomly selected endogeneous granules for passive, round neutrophils. *Inset*: typical trajectory of the centroid of a granule used to calculate the MSD. *D*: individual MSD traces of randomly selected endogeneous granules for neutrophils that have undergone deformation into a microchannel. *Inset*: typical trajectory of the centroid of a granule used to calculate the MSD. *E*: typical plot of average MSD curves for neutrophils before and after exposure to mechanical stimulation.

and height of 1.5 μm. The effective diameter of the microchannels was calculated using the relationship effective diameter = $\sqrt{4WH/\pi}$, where W is width and H is height, hence, giving us effective diameters of 4.0 and 3.1 μm, denoted by D_L and D_S, respectively. Most experiments were carried out at 37°C, but some were also conducted at 23°C to examine the temperature-dependent behavior of the cell. We found experimentally that the threshold pressure for the cell to successfully deform into the microchannels was ~0.4 mmH_2O for D_L, and ~2 mmH_2O for D_S. Therefore, different pressure ranges (ΔP) were used for the two channels: ΔP = 1, 10, and 50 mmH_2O for D_L; ΔP = 10 and 50 mmH_2O for D_S. The values of ΔP chosen were above the threshold pressure for the respective channel diameters but within physiological limits experienced by neutrophils in pulmonary capillaries (16).

Typical trajectories of the granules, individual mean-square displacements, and average mean-square displacement plots for neutrophils before and after mechanical deformation are shown in Fig. 5, *C–E*. A representative sequence of events during neutrophil deformation, followed by trapping and, ultimately, pseudopod formation is depicted in Fig. 6. The location of pseudopod projection occurred randomly (either at the leading or trailing edge of the cell but never at both sites). After pseudopod formation, the cell would begin to crawl along the microchannel in the direction of the pseudopod protrusion.

An increase in ΔP resulted in a decrease in entrance time (Fig. 7) as evidenced, for example, by comparing the data for D_L, 1 mmH_2O, 37°C, and D_L, 10 mmH_2O, 37°C. Increasing the cross-sectional area of the microchannel produced a similar effect (D_S, 10 mmH_2O, 37°C, vs. D_L, 10 mmH_2O, 37°C), as was the case when the temperature was raised from 23 to 37°C (e.g., D_L, 1 mmH_2O, 23°C vs. D_L, 1 mmH_2O, 37°C).

The time to pseudopod formation is shown in Fig. 8 for different experimental conditions. Pseudopods were observed for D_L, 1 mmH_2O and D_L, 10 mmH_2O at 37°C, but not for similar conditions at 23°C. Only when ΔP was raised to 50 mmH_2O for the case of D_L, 23°C, was pseudopod projection observed, and then only after ~100 s from the time of cell entry into the channel. For D_L, 1 mmH_2O, 23°C and D_L, 10 mmH_2O, 23°C, no pseudopod projection was observed even though the cells were monitored for >10 min.

Because the time to pseudopod activation varied with temperature, we focused on the conditions at 37°C to examine the effect of entrance time. Comparison of experiments carried out at 37°C (Fig. 9) showed a clear inverse correlation between deformation rate (computed as the inverse of entrance time)

Journal of Applied Physiology

Downloaded from jap.physiology.org on December 27, 2005

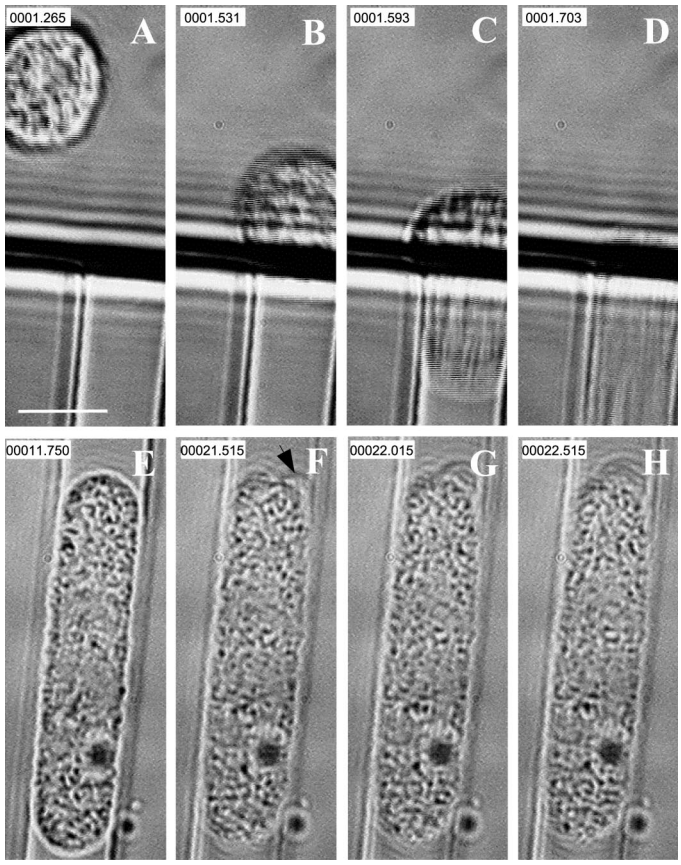

Fig. 6. Image sequence showing a neutrophil flowing toward the microchannel entrance (*A*), the leading edge of the cell just crossing the channel inlet (*B*), the cell undergoing deformation (*C*), the trailing edge of fully deformed cell just clearing the channel mouth (*D*), and subsequently, the neutrophil was trapped in the channel (*E*). After some time, the cell can be seen to form a pseudopod projection (*F–H*). Arrow *F* points to the location at the trailing edge of the cell where pseudopod protrusion was first seen. Here, the neutrophil was flowing into an effective diameter of 4.0 μm (D_L) under a pressure difference of 50 mmH_2O at 37°C. Scale bar, 5 μm.

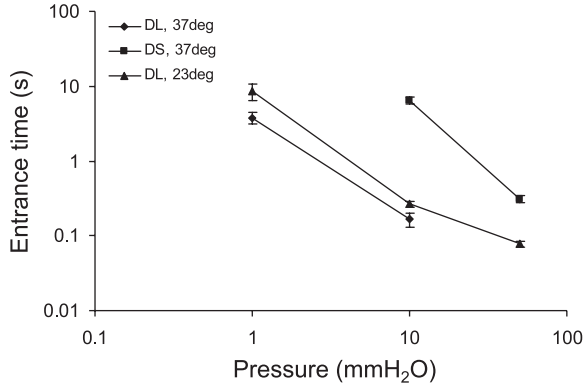

Fig. 7. Entrance time for different experimental conditions. Data are expressed as means ± SE. Number of observations for the corresponding experimental conditions are as follows: D_L, 1 mmH_2O, 37°C ($n = 8$); D_L, 10 mmH_2O, 37°C ($n = 8$); D_S, 10 mmH_2O, 37°C ($n = 4$); D_S, 50 mmH_2O, 37°C ($n = 4$); D_L, 1 mmH_2O, 23°C ($n = 5$); D_L, 10 mmH_2O, 23°C ($n = 8$); D_L, 50 mmH_2O, 23°C ($n = 6$)

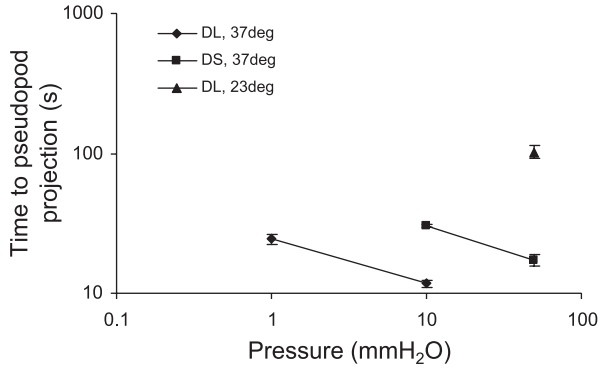

Fig. 8. Time to pseudopod projection for different experimental conditions. Data are means ± SE. *n* Values for the corresponding experimental conditions are as follows: D_L, 1 mmH_2O, 37°C ($n = 5$); D_L, 10 mmH_2O, 37°C ($n = 8$); D_S, 10 mmH_2O, 37°C ($n = 4$); D_S, 50 mmH_2O, 37°C ($n = 4$); D_L, 50 mmH_2O, 23°C ($n = 5$). Not shown in the figure are data for D_L, 1 mmH_2O, 23°C ($n = 5$) and D_L, 10 mmH_2O, 23°C ($n = 6$), in which no pseudopod projection was observed even though the cells were monitored for at least 10 min.

and the time of pseudopod formation. These results suggest that neutrophil activation, as reflected by pseudopod formation, will occur more rapidly when neutrophils are subjected to a higher rate of deformation.

To investigate the effects of mechanical deformation on the viscoelastic properties of neutrophils, we used the multiple-particle-tracking method. The technique was first applied to adherent and spread neutrophils (Fig. 5*B*). Measurements at 1 Hz (see Table 1) revealed a G′ of 43.8 ± 5.0 dyn/cm^2 and η of 2.2 ± 0.3 $dyn \cdot s \cdot cm^{-2}$. Round, passive neutrophils introduced into the glass-slide coverslip chamber and allowed to settle on the coverslip were also studied. Due to the presence of plasma in their surrounding medium, the majority of the neutrophils (~98%) remained round (Fig. 5*A*) and free of pseudopod projection. Some of these adhered nonspecifically to the coverslip, whereas the rest floated loosely at the bottom of the chamber. Because the round, adherent cells remained stationary, they were chosen for particle tracking. The viscoelastic values of neutrophils were G′ = 242 ± 21 dyn/cm^2 and G″ = 470 ± 40 $dyn \cdot cm^{-2}$ at 37°C, as summarized in Table 1. These values were significantly lower ($P < 0.05$) than the viscoelastic moduli at 23°C (G′ = 303 ± 19 dyn/cm^2 and G″ = 649 ± 55 $dyn \cdot cm^{-2}$), highlighting the effect of temperature on the mechanical properties of the cell.

To study the effect of mechanical deformation on the viscoelastic properties of neutrophils, particle tracking was performed once the cells had entered the microchannel. The experiments were carried out at 37°C. The motion of neutro-

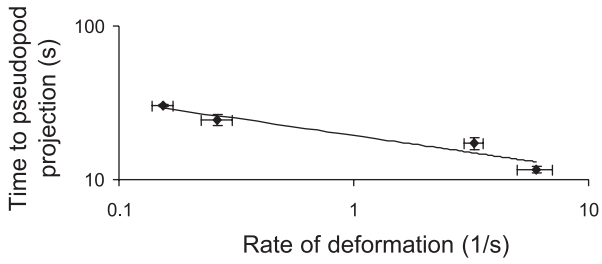

Fig. 9. Effect of rate of deformation on time to pseudopod projection for neutrophils at 37°C.

Journal of Applied Physiology

Downloaded from jap.physiology.org on December 27, 2005

Table 1. *Measurements of G′, G″, and G″/G′*

	G′, dyn/cm^2	G″, dyn/cm^2	G″/G′
Adherent, spreading neutrophil, 37°C (n = 4; N = 70)	44	14	0.32
Passive, round neutrophil, 37°C (n = 4; N = 51)	242	470	1.9
Passive, round neutrophil, 23°C (n = 4; N = 71)	303	649	2.1

Elastic modulus (G′), loss modulus (G″), and their ratio (G″/G′), at 1 Hz, of adherent spread neutrophils at 37°C and passive, round neutrophils at 37°C and 23°C. *n,* Number of cells; *N,* number of granules.

phil granules was monitored as soon as the cell was immobilized and the image focused. Tracking continued until the first observation of pseudopod projection, beyond which the cell began to crawl and granular motion became erratic, complicating the analysis. The temporal changes in G′ and G″ for the different flow conditions are shown in Figs. 10 and 11, respectively. With the use of values obtained for passive, round neutrophils (Table 1) as controls, the data show that mechanical deformation causes a significant drop ($P < 0.05$) in G′ and G″. For all flow conditions, the mean value of G′ was reduced by ~50–60% from its predeformation value of 242 dyn/cm^2. Similarly, the mean value of G″ was reduced by ~35–50% after deformation. Interestingly, although mechanical deformation resulted in a softer and less viscous cytoplasm, the drop in magnitude of G′ and G″ was quantitatively similar and independent of the degree of deformation. For the flow conditions of D_L at 1 (37°C) and 10 mmH$_2$O (37°C) and D_S at 50 mmH$_2$O (37°C), the cell maintained the softer, lower G″ until pseudopod projections appeared. However, for the flow condition of D_S at 10 mmH$_2$O (37°C) after the initial drop, G′ and G″ were seen to recover to roughly their predeformation values before pseudopod projection. This flow condition corresponded to the case of lowest rate of deformation in Fig. 9.

Although quantitative particle tracking was not possible once the neutrophils begin to crawl, observation of random granule motion of the neutrophils showed periodic cycling of enhanced and reduced motion paralleling the cyclic projection of pseudopods during cell locomotion. The granules at the pseudopod leading edge were seen to have increased activity when a new wave of granules first flowed into the pseudopod; however, the granule activity soon diminished and remained low even during the next cycle of pseudopod projection. Only after the new pseudopod had fully extended would granular motion increase again when the next wave of granules entered the newly formed pseudopod. These observations are consistent with those seen in neutrophils locomoting on a flat substrate (37).

DISCUSSION

This study provides direct evidence that mechanical force of a magnitude comparable to that encountered by a neutrophil during transit through the microcirculation exerts a strong and fundamental effect on cell structure and function. The consequences of mechanical stimulation are immediate, occurring within seconds of stimulation, and substantial. A drop in shear modulus by >60% is observed within seconds of entering a constriction, independent of magnitude of the stimulus. In contrast, pathways leading to migratory behavior are excited in a strain rate-dependent manner, suggesting that these two phenomena may be independently controlled. Taken together, these results suggest an important role for mechanical stimu-

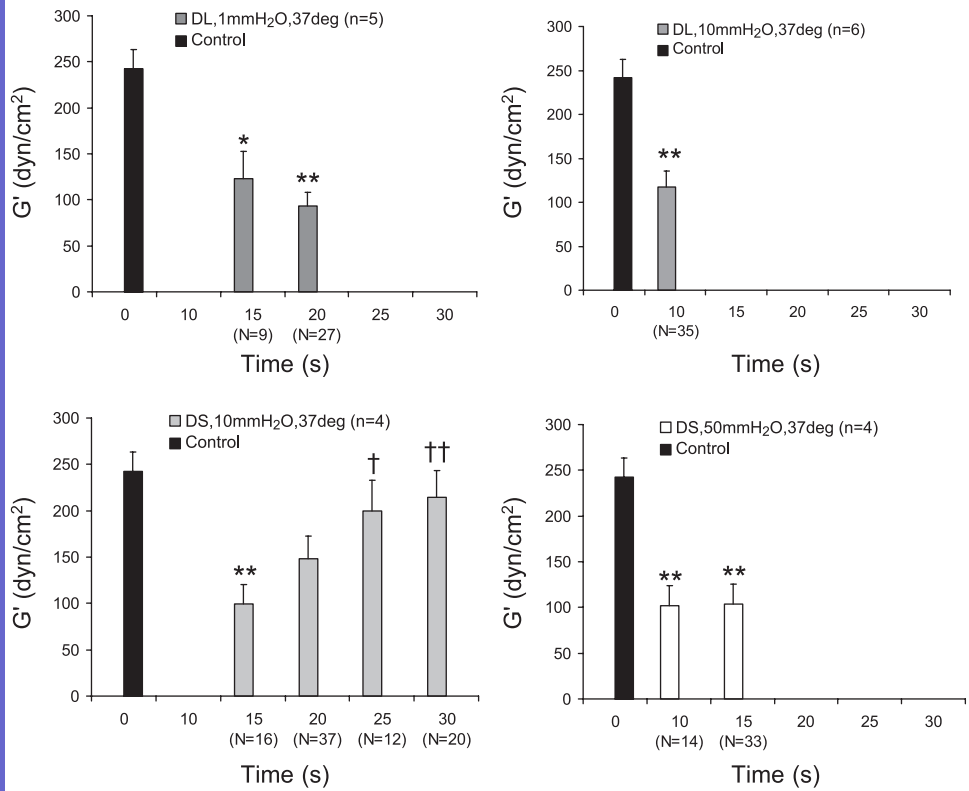

Fig. 10. Temporal change in elastic modulus (G′) of neutrophil after mechanical deformation into a microchannel at a lag time of 0.03 s. Graphs show changes in G′ under different flow conditions at 37°C. Time = 0 s represents the instance when the leading edge of the cell had just crossed the channel inlet. The time at which G′ could first be recorded varied due to dissimilar entrance time for the different flow conditions. Value of G′ for passive, round neutrophils at 37°C (Table 1) serves as control. Data are means ± SE. n, Number of cells; N, no. of granules. *$P <$ 0.05 and **$P < 0.01$ compared with control; †$P < 0.05$ and ††$P < 0.01$ compared with data at time = 15 s.

Journal of Applied Physiology

Downloaded from jap.physiology.org on December 27, 2005

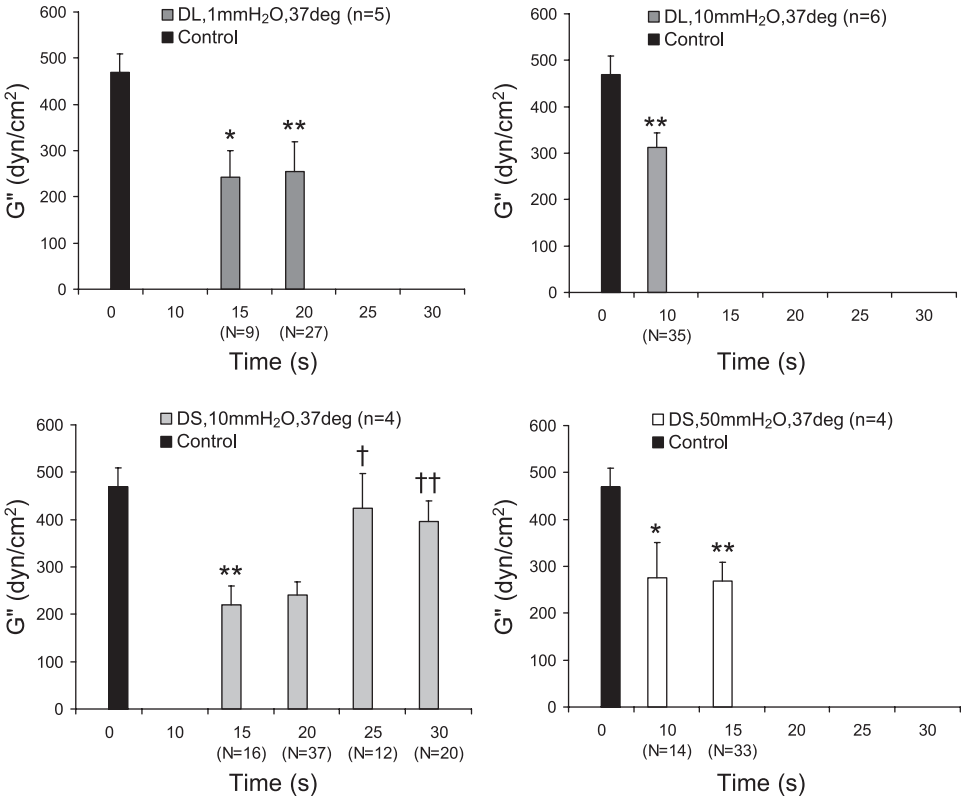

Fig. 11. Temporal change in loss modulus (G″) of neutrophil after mechanical deformation into a microchannel at a lag time of 0.03 s. Graphs show changes in G″ under different flow conditions at 37°C. Time = 0 s represents the instance when the leading edge of the cell had just crossed the channel inlet. The time at which G″ could be first recorded varied due to dissimilar entrance time for the different flow conditions. Value of G″ for passive, round neutrophils at 37°C (Table 1) serves as control. Data are means ± SE. *$P < 0.05$ and **$P < 0.01$ compared with control; †$P < 0.05$ and ††$P < 0.01$ compared with data at time = 15 s.

lation of neutrophils, influencing both their rheology and their migratory tendencies.

The combination of microfabrication and particle tracking microrheology allowed us to simultaneously visualize and quantify the response of neutrophils. Previous studies of neutrophil deformation have been conducted using in vitro filtration (7, 21, 31) or micropipette aspiration (6, 30). In the former, large cell numbers enabled studies of changes in deformabilities and biochemical analysis of the changes in F-actin content and free intracellular Ca^{2+} concentration, for example, but direct rheological measurements were not possible. Micropipette experiments provide data on cell rheology, determined from entrance times, but provide limited data on time-dependent changes in viscoleastic properties or changes in specific cell constituents. Analysis of the thermal motions of endogenous granules would be difficult in this situation due to the requirement of high-resolution optics. In particular, methods used previously to infer rheological properties from micropipette aspiration times assume that the rheological parameters are constant in time and unaffected by the mechanical forces imposed during manipulation of the cell. Our results suggest that this may not be a valid assumption.

The microfluidic device was coupled to a macrofluidic system consisting of a set of reservoirs. Pressure difference was imposed across the microchannel by varying the height of water in the reservoirs. The threshold pressure (ΔP_{thr}) for D_L and D_S in the experiment was compared with the theoretical expression $\Delta P_{thr} = 4\gamma[(1/D_{pipette}) - (1/D_{cell})]$, where $D_{pipette}$ is the diameter of the pipette, D_{cell} is the cell diameter, and the cell cortical tension ($\gamma = 35$ pN/μm) has been measured previously (39). Due to the rectangular cross section used in the present experiments, we can make only an approximate comparison by substituting effective diameter for $D_{pipette}$. Doing so, we find that the experimentally measured values of ΔP_{thr} (0.4 and 2.0 mmH_2O for the large and small channels, respectively) are somewhat lower than the theoretically predicted values of 1.9 and 2.7 mmH_2O, but this difference could be attributable to the different cross-sectional shape or entrance geometry. In contrast, entrance times observed in the present experiments were ~40 times smaller than those reported in the literature for micropipette aspiration under similar driving pressures and diameters. Cross-sectional shape might also influence entrance times, but the entrance geometry also likely contributes. Previous numerical simulations have shown that entrance times depend strongly on the axial radius of curvature of the entrance (1). This would be consistent with the observation that the entrance to our microchannels tends to be somewhat more rounded than that of a micropipette. However, aside from a slight lowering of the threshold pressure and shorter entrance times, the effects of driving pressure, channel cross-sectional area, and temperature (Fig. 7) are generally consistent with previously published results (8).

Mechanical deformation of neutrophils into the pulmonary capillaries induced pseudopod formation for all experimental conditions at 37°C but only at the higher values of ΔP for experiments at 23°C (Fig. 8). Comparing similar experimental conditions, it took considerably longer for pseudopod projection at the lower temperature (10–30 s at 37°C and ~100 s at 23°C). Furthermore, the results indicate that, for a given temperature, the time to pseudopod projection is inversely correlated to the rate of deformation of the neutrophil (Fig. 9), which we use here as a measure of the stimulus magnitude. These results are consistent with observations of activation reported in a previous micropipette aspiration study (8) that

Journal of Applied Physiology

Downloaded from jap.physiology.org on December 27, 2005

reported a transition from passive to active motile state, with activation time varying between 0 and 120 s at 37°C and between 60 and 120 s at 23°C. Hence, our results confirm that mechanical deformation is not a passive event; rather, it leads to neutrophil activation with pseudopod formation if the stimulus is sufficiently large. Above the threshold stimulus, it appears that the time required for activation is dependent on the rate of deformation experienced by the cell, implying the existence of a mechanosensing or signal transduction mechanism in the cell that is able to modulate the response according to the magnitude of the mechanical stimulus. In contrast, we found that neutrophil entrance time behaved in a manner more consistent with a passive cell in that it was determined primarily by the initial value of the shear modulus, which was only slightly dependent on temperature. (Fig. 7).

Our measurements of viscoelastic moduli of adherent, spread neutrophils obtained using the particle tracking system (Table 1) can be compared with published results of Yanai et al. (37), who reported mean values of $G' = \sim 10$ dyn/cm^2 and viscosity $\eta = \sim 4.0$ dyn·s/cm^2 for the body and trailing region of the neutrophil using an optical trap to excite the granules at frequencies between 0.3 and 3 Hz. Our measurements for η matched closely with the previously published results, whereas the value for G' was about four times higher. One potential explanation for this difference is that the optical trap technique was capable of measuring only those granules that were freely moving, whereas other particles were too stiff to be oscillated at maximum laser power.

Table 1 also shows the ratio of G'' to G' for the measurements carried out on adherent, spread neutrophils and those for passive, round cells at 37 and 23°C. Our value of G''-to-G' ratio of 0.32 for adherent, spread neutrophils matches the value of ~0.3 obtained at 0.75 Hz using magnetic twisting cytometry (10). However, there are no similar figures reported in the literature for passive, round cells. Nevertheless, the values of G''-to-G' ratio of ~2.0 for passive, round cells is within the limits of the values (0.25–20) reported for other cell types using various experimental techniques (10, 34, 36).

To gain further insight into the effects of mechanical deformation on the cytoskeletal structure of the neutrophil, the granules of the neutrophils were tracked to monitor the change in rheology of the cell before and after deformation. Mechanical deformation results in a reduction in elastic moduli by 50–60%, within 10–15 s after the initial stimulus, from its value as a passive, round cell before deformation (Figs. 10 and 11). Similarly, the loss moduli drop by 35–50% from the unactivated values of the cells. These data demonstrate that mechanical deformation causes either disruption or remodeling of the neutrophil cytoskeleton. In view of the decrease in viscoelastic properties of the cell, this might be due either to a sudden depolymerization of filamentous actin or rupture of cross-links bridging between actin filaments. The lack of a significant temperature effect on entrance time, in combination with the short time scale of the modulus changes (~10 s), leads us to favor the theory that the rapid deformation ruptures actin cross-links. In contrast, Kitagawa and coworkers (21) observed an immediate but short-lived increase in F-actin, leading them to conclude that mechanical deformation resulted in an increase in actin cross-linking events rather than actin polymerization. Further experiments are required to reconcile these seemingly contradictory results.

Another interesting observation is that the magnitude of drop in the values of G' and G'' after deformation was found to be independent of the degree of deformation. This is in contrast with the time to pseudopod formation, which correlates with the rate of deformation. Also, neutrophils subjected to low deformation rates were observed to recover much of their modulus reduction within ~30 s and return nearly to their initial mechanical state. These data suggest that the extent of depolymerization or loss of actin cross-linking is similar regardless of the magnitude or rate of deformation, at least within the range of these experiments, but the initiation of actin polymerization to form pseudopods is dependent on the magnitude of force transduced. One scenario consistent with these observations is that the large strain deformations effectively shear and rupture many of the actin cross-links, leaving them attached to one filament but displaced relative to their initial cross-linking site. Once the deformation stops, these cross-links can reform but do so in the new, deformed state, returning the cell to its initial mechanical state but in a new, deformed geometry. Thus it appears that the molecular mechanism controlling the depolymerization/actin cross-link breakdown is separate from the mechanism governing pseudopod formation and viscoelastic recovery; however, further experiments would be needed to confirm this.

This evidence of viscoelastic recovery could help explain results from neutrophil recovery experiments after deformation into micropipettes (32). In that study, neutrophils were aspirated fully into a micropipette and held for various periods of time before being expelled. Cells held in the micropipette for a short time (<5 s) exhibited a rapid elastic rebound immediately after being expelled from the pipette. In contrast, neutrophils held for longer times (>5 s) displayed a smoother recovery and took much longer to recover to their spherical shape (~75 s to reach 90% of its full recovery compared with ~55 s for the short holding time). These observations can be explained on the basis of the rapid fall and slower recovery of modulus after deformation observed in the present experiments. Cells ejected immediately after being aspirated would have a low internal modulus and few cross-links; thus their surface tension could rapidly return the cell to a spherical shape. Cells held for a longer period would remodel due to reformation of actin cross-links; on ejection, the cell would need to remodel once again but this time under the action of a much smaller restoring force that was due to surface tension alone.

We recognize that the multiple particle tracking technique used in this investigation has limitations, especially compared with the recently developed method of two-particle microrheology (4, 11). In multiple particle tracking, granule size must be estimated, introducing error (a factor of ~2) into the viscoelastic modulus obtained. In two-particle microrheology, the cross-correlated motion of pairs of particles is independent of particle size and shape and is unaffected by the coupling between the particles and the medium. Unfortunately, measurement by the two-particle technique requires data collection over a much longer period of time than the multiple particle tracking method, hence preventing us from monitoring temporal changes in the cell. The two-particle microrheology technique is more suitable for measurements where the behavior of the cells is relatively unchanged over the period of data collection (25). Thus we resort to the multiple particle tracking method in the present study, and in the application of this technique, we

Journal of Applied Physiology

Downloaded from jap.physiology.org on December 27, 2005

maximized the accuracy of the results by eliminating granules that are not circular and also by selecting granules of almost equal size. Because active motion can only cause an apparent reduction in modulus (greater granular motion), however, these results represent a lower bound on modulus.

In summary, this study shows that mechanical deformation of neutrophils into pulmonary capillaries results in activation of the cell by inducing cytoskeletal remodeling, leading to changes in viscoelastic properties and pseudopod projection. Hence, mechanical deformations are capable of activating a neutrophil, providing a migratory stimulus and thereby enhancing their tendency to transmigrate across the endothelium.

APPENDIX

The design of the microchannel was drawn in AutoCAD (Autodesk, San Rafael, CA) for fabrication on chromium masks (Photronics, Brookfield, CT) (Fig. 1). The fabrication of the master utilized the technique of two-level photolithography. Silicon wafers [100 mm, 425–525 μm, 1–10 Ω (1-0-0); Transition Technology International, Sunnyvale, CA] were spin-coated with the first layer of SU-8 2002 photoresist (Microchem, Newton, MA) to a thickness of either 1.5 or 2.5 μm, and prebaked at 95°C for 2 min. The resist was then exposed to ultraviolet light with an intensity of 10 mW/cm^2 for 11.5 s through the first chromium mask with features of the microchannel and the reservoirs. The resist was postbaked at 95°C for 2 min, which cross-linked the regions exposed to ultraviolet light. Next, a second layer of SU-8 2010 photoresist was spin-coated to a thickness of 15 μm on top of the first layer, followed by prebaking at 95°C for 4 min. The second chromium mask with features of the reservoirs only was aligned, and the photoresist was exposed for 20 s. After postbaking again at 95°C for 3 min, SU-8 developer (Microchem) was used for 5 min to develop the features in both resist layers. Finally, the height of the microchannel was checked with a profilometer (Dektak 2, Veeco Instruments, Woodbury, NY).

When the master was successfully fabricated, the device was formed in PDMS by replica molding. The master of photoresist was first treated with trimethylchlorosilane (Sigma-Aldrich, St. Louis, MO) to prevent adhesion of PDMS to the master after curing. A curing agent and PDMS prepolymer (SYLGARD 184 Silicone Elastomer Kit, Dow Corning, Midland, MI) were mixed together and degassed for 5 min to remove air bubbles. The mixture was then poured onto the master and cured in an oven at 80°C for 3 h. When cured, the PDMS was removed by peeling off the master. Inlet and outlet reservoir ports were formed by punching the PDMS with a 16-gauge adapter needle. Through these bored tunnels, inlet and outlet tubes would later be inserted, which allowed connection of the microfluidic device to the external macrofluidic system.

The final step involved sealing the PDMS to a glass coverslip. The coverslip was also spin-coated with a thin layer of the same PDMS elastomer and cured in the oven. Both the microdevice and the coverslip were subjected to plasma oxidation for 30 s (Plasma Cleaner, Harrick Scientific, Ossining, NY), after which the surfaces were brought together to form an irreversible seal and produce the finished device (Fig. 2).

ACKNOWLEDGMENTS

The authors thank Thierry Savin and Patrick S. Doyle for assistance with particle tracking, Jorge M. Ferrer and Matthew J. Lang for microscopy assistance, and Hayden Huang for cell preparation.

GRANTS

Support from the National Heart, Lung, and Blood Institute (P01 HL-64858), a Whitaker Foundation Graduate Student Fellowship, and National University of Singapore Overseas Graduate Scholarship (to B. Yap) is gratefully acknowledged.

REFERENCES

1. **Bathe M, Shirai A, Doerschuk CM, and Kamm RD.** Neutrophil transit times through pulmonary capillaries: the effects of capillary geometry and fMLP-stimulation. *Biophys J* 83: 1917–1933, 2002.
2. **Coughlin MF and Schmid-Schonbein GW.** Pseudopod projection and cell spreading of passive leukocytes in response to fluid shear stress. *Biophys J* 87: 2035–2042, 2004.
3. **Crocker JC and Grier DG.** Methods of digital video microscopy for colloidal studies. *J Colloid Interface Sci* 179: 298–310, 1996.
4. **Crocker JC, Valentine MT, Weeks ER, Gisler T, Kaplan PD, Yodh AG, and Weitz DA.** Two-point microrheology of inhomogeneous soft materials. *Phys Rev Lett* 85: 888–891, 2000.
5. **Doerschuk CM, Beyers N, Coxson HO, Wiggs B, and Hogg JC.** Comparison of neutrophil and capillary diameters and their relation to neutrophil sequestration in the lung. *J Appl Physiol* 74: 3040–3045, 1993.
6. **Dong C, Skalak R, and Sung KLP.** Cytoplasmic rheology of passive neutrophils. *Biorheology* 28: 557–567, 1991.
7. **Downey GP, Doherty DE, Schwab B, Elson EL, Henson PM, and Worthen GS.** Retention of leukocytes in capillaries—role of cell-size and deformability. *J Appl Physiol* 69: 1767–1778, 1990.
8. **Evans E and Kukan B.** Passive material behavior of granulocytes based on large deformation and recovery after deformation tests. *Blood* 64: 1028–1035, 1984.
9. **Evans E and Yeung A.** Apparent viscosity and cortical tension of blood granulocytes determined by micropipet aspiration. *Biophys J* 56: 151–160, 1989.
10. **Fabry B, Maksym GN, Butler JP, Glogauer M, Navajas D, and Fredberg JJ.** Scaling the microrheology of living cells. *Phys Rev Lett* 87: 148102-1–148102-4, 2001.
11. **Gardel ML, Valentine MT, Crocker JC, Bausch AR, and Weitz DA.** Microrheology of entangled F-actin solutions. *Phys Rev Lett* 91: 158302, 2003.
12. **Gebb SA, Graham JA, Hanger CC, Godbey PS, Capen RL, Doerschuk CM, and Wagner WW.** Sites of leukocyte sequestration in the pulmonary microcirculation. *J Appl Physiol* 79: 493–497, 1995.
13. **Hogg JC.** Neutrophil kinetics and lung injury. *Physiol Rev* 67: 1249–1295, 1987.
14. **Hogg JC, Coxson HO, Brumwell ML, Beyers N, Doerschuk CM, Macnee W, and Wiggs BR.** Erythrocyte and polymorphonuclear cell transit-time and concentration in human pulmonary capillaries. *J Appl Physiol* 77: 1795–1800, 1994.
15. **Huang HD, Kamm RD, and Lee RT.** Cell mechanics and mechanotransduction: pathways, probes, and physiology. *Am J Physiol Cell Physiol* 287: C1–C11, 2004.
16. **Huang YQ, Doerschuk CM, and Kamm RD.** Computational modeling of RBC and neutrophil transit through the pulmonary capillaries. *J Appl Physiol* 90: 545–564, 2001.
17. **Ingber DE.** Mechanobiology and diseases of mechanotransduction. *Ann Med* 35: 564–577, 2003.
18. **Jo BH, Van Lerberghe LM, Motsegood KM, and Beebe DJ.** Three-dimensional micro-channel fabrication in polydimethylsiloxane (PDMS) elastomer. *J Microelectromech Sys* 9: 76–81, 2000.
19. **Jo S and Park K.** Surface modification using silanated poly(ethylene glycol)s. *Biomaterials* 21: 605–616, 2000.
20. **Juncker D, Schmid H, Bernard A, Caelen I, Michel B, de Rooij N, and Delamarche E.** Soft and rigid two-level microfluidic networks for patterning surfaces. *J Micromech Microengin* 11: 532–541, 2001.
21. **Kitagawa Y, VanEeden SF, Redenbach DM, Daya M, Walker BAM, Klut ME, Wiggs BR, and Hogg JC.** Effect of mechanical deformation on structure and function of polymorphonuclear leukocytes. *J Appl Physiol* 82: 1397–1405, 1997.
22. **Kitayama J, Hidemura A, Saito H, and Nagawa H.** Shear stress affects migration behavior of polymorphonuclear cells arrested on endothelium. *Cell Immunol* 203: 39–46, 2000.
23. **Kole TP, Tseng Y, Huang L, Katz JL, and Wirtz D.** Rho kinase regulates the intracellular micromechanical response of adherent cells to rho activation. *Mol Biol Cell* 15: 3475–3484, 2004.
24. **Kole TP, Tseng Y, Jiang I, Katz JL, and Wirtz D.** Intracellular mechanics of migrating fibroblasts. *Mol Biol Cell* 16: 328–338, 2005.
25. **Lau AWC, Hoffman BD, Davies A, Crocker JC, and Lubensky TC.** Microrheology, stress fluctuations, and active behavior of living cells. *Phys Rev Lett* 91: 2003.

Journal of Applied Physiology

Downloaded from jap.physiology.org on December 27, 2005

26. **Mason TG, Ganesan K, van Zanten JH, Wirtz D, and Kuo SC.** Particle tracking microrheology of complex fluids. *Phys Rev Lett* 79: 3282–3285, 1997.
27. **McDonald JC, Duffy DC, Anderson JR, Chiu DT, Wu HK, Schueller OJA, and Whitesides GM.** Fabrication of microfluidic systems in poly-(dimethylsiloxane). *Electrophoresis* 21: 27–40, 2000.
28. **Moazzam F, Delano FA, Zweifach BW, and Schmidschonbein GW.** The leukocyte response to fluid stress. *Proc Natl Acad Sci USA* 94: 5338–5343, 1997.
29. **Needham D and Hochmuth RM.** Rapid flow of passive neutrophils into a 4 Mu-M pipette and measurement of cytoplasmic viscosity. *J Biomech Eng* 112: 269–276, 1990.
30. **Schmid-Schonbein GW, Sung KLP, Tozeren H, Skalak R, and Chien S.** Passive mechanical-properties of human-leukocytes. *Biophys J* 36: 243–256, 1981.
31. **Selby C, Drost E, Wraith PK, and Macnee W.** In vivo neutrophil sequestration within lungs of humans is determined by in vitro filterability. *J Appl Physiol* 71: 1996–2003, 1991.
32. **Transontay R, Needham D, Yeung A, and Hochmuth RM.** Time-dependent recovery of passive neutrophils after large deformation. *Biophys J* 60: 856–866, 1991.
33. **Tsai MA, Frank RS, and Waugh RE.** Passive mechanical-behavior of human neutrophils—power-law fluid. *Biophys J* 65: 2078–2088, 1993.
34. **Tseng Y and Wirtz D.** Mechanics and multiple-particle tracking micro-heterogeneity of alpha-actinin-cross-linked actin filament networks. *Biophys J* 81: 1643–1656, 2001.
35. **Whitesides GM, Ostuni E, Takayama S, Jiang XY, and Ingber DE.** Soft lithography in biology and biochemistry. *Annu Rev Biomed Eng* 3: 335–373, 2001.
36. **Yamada S, Wirtz D, and Kuo SC.** Mechanics of living cells measured by laser tracking microrheology. *Biophys J* 78: 1736–1747, 2000.
37. **Yanai M, Butler JP, Suzuki T, Kanda A, Kurachi M, Tashiro H, and Sasaki H.** Intracellular elasticity and viscosity in the body, leading, and trailing regions of locomoting neutrophils. *Am J Physiol Cell Physiol* 277: C432–C440, 1999.
38. **Yanai M, Butler JP, Suzuki T, Sasaki H, and Higuchi H.** Regional rheological differences in locomoting neutrophils. *Am J Physiol Cell Physiol* 287: C603–C611, 2004.
39. **Yeung A and Evans E.** Cortical shell-liquid core model for passive flow of liquid-like spherical cells into micropipets. *Biophys J* 56: 139–149, 1989.

Journal of Applied Physiology
Downloaded from jap.physiology.org on December 27, 2005